OCL
Oilseeds & fats Crops and Lipids

Available online at:
www.ocl-journal.org

RESEARCH ARTICLE – DOSSIER

OPEN ACCESS

DOSSIER

LIPIDS AND BRAIN
LIPIDES ET CERVEAU

Selective comparison of gelling agents as neural cell culture matrices for long-term microelectrode array electrophysiology

Nicolai Wilk[1,2], Rouhollah Habibey[1], Asiyeh Golabchi[1,3], Shahrzad Latifi[1,4], Sven Ingebrandt[2] and Axel Blau[1,*]

[1] Italian Institute of Technology (IIT), Dept. of Neuroscience and Brain Technologies (NBT), via Morego 30, 16163 Genoa, Italy
[2] Dept. of Informatics and Microsystem Technology, University of Applied Sciences Kaiserslautern, Amerikastraße 1, 66482 Zweibrücken, Germany
[3] Dept. of Bioengineering, University of Pittsburgh, 3501 Fifth Avenue, Pittsburgh, PA 15260, USA
[4] David Geffen School of Medicine at UCLA, Dept. of Neurology, 635 Charles E. Young, Los Angeles, CA 90095, USA

Abstract – In classic monolayer cell culture, the world is flat. In contrast, tissue-embedded cells experience a three-dimensional context to interact with. We assessed a selection of natural gelling agents of non-animal origin (ι- and κ-carrageenan, gellan gum, guar gum, locust bean gum, sodium alginate, tragacanth and xanthan gum) in serum-free medium at 1–4% (w/v) concentration for their suitability as a more natural 3D culture environment for brain-derived cells. Their biophysical properties (viscosity, texture, transparency, gelling propensity) resemble those of the extracellular matrix (ECM). Gels provide the neurons with a 3D scaffold to interact with and allow for an increase of the overall cell density compared to classical monolayer 2D culture. They not only protect neurons in cell culture from shear forces and medium evaporation, but stabilize the microenvironment around them for efficient glial proliferation, tissue-analog neural differentiation and neural communication. We report on their properties (viscosity, transparency), their ease of handling in a cell culture context and their possible use modalities (cell embedment, as a cell cover or as a cell culture substrate). Among the selected gels, guar gum and locust bean gum with intercalated laminin allowed for cortical cell embedment. Neurons plated on and migrating into gellan gum survived and differentiated even without the addition of laminin. Sodium alginate with laminin was a suitable cell cover. Finally, we exemplarily demonstrate how guar gum supported the functional survival of a cortical culture over a period of 79 days in a proof-of-concept long-term microelectrode array (MEA) electrophysiology study.

Keywords: Microbial-, plant- and algae-derived gelling agents / 3D neural cell culture / microelectrode array electrophysiology

Résumé – Comparaison sélective d'agents gélifiants utilisés en tant matrices de cultures de cellules neurales en 3 dimensions pour une approche à long terme d'électrophysiologie. Au contraire de la culture classique pratiquée en monocouche (2D), la culture cellulaire en 3 dimensions (3D) permet de reproduire les interactions entre cellules d'un tissu. Nous avons évalué une sélection d'agents gélifiants naturels d'origine non animale (ι- et κ-carraghénane, gomme gellane, gomme de guar, gomme de caroube, alginate de sodium, gomme adragante et gomme de xanthane) dans un milieu sans sérum à des concentrations de 1–4 % (w/v) au regard de leur aptitude à offrir un milieu de culture 3D plus naturel pour les cellules cérébrales. Les propriétés biophysiques de ces agents (viscosité, texture, transparence, propension de gélification) ressemblent à celles de la matrice extracellulaire. Les gels fournissent aux neurones un assemblage 3D pour interagir et permettre une augmentation de la densité cellulaire globale, comparativement à une culture monocouche 2D classique. Ils protègent non seulement les neurones en culture cellulaire des forces de cisaillement et de l'évaporation moyenne, mais stabilisent également le micro-environnement qui les entoure, assurant ainsi l'efficacité de la prolifération des cellules gliales, de la différenciation et de la communication neuronales. Cet article rapporte donc des données sur leurs propriétés (viscosité, transparence), leur facilité de manipulation en culture cellulaire et leurs modalités d'utilisation possibles (enrobage de la cellule, en tant que couvercle cellulaire ou en tant que substrat de la culture cellulaire). Parmi les gels sélectionnés, la gomme de guar et la gomme de caroube, avec de la laminine intercalée, permettent l'enrobage de cellules corticales. Les neurones étalés et migrant dans la gomme de gellane survivent et se différencient même sans l'addition de laminine. L'alginate de sodium additionné de

---

* Correspondence: axel.blau@iit.it

laminine forme un couvercle cellulaire approprié. Enfin, nous démontrons de manière univoque comment la gomme de guar a permis la survie d'une culture fonctionnelle corticale sur une période de 79 jours dans le cadre d'une étude de concept d'électrophysiologie à long terme avec une matrice de microélectrodes.

Mots clés : Gélifiants, d'origine microbienne, de plantes et d'algues / culture cellulaire neurale 3D / matrice de microélectrodes d'électrophysiologie

1 Introduction

Most *in vitro* culture models of adherent mammalian cells are two-dimensional. With most of the body's supply (*e.g.*, vascular system) and signaling infrastructure missing, cells usually populate the substrate surface in a density-dependent manner, but rarely expand into the vertical dimension. They therefore adapt their morphology and function to this non-natural environment. Consequently, the physiology of such 2D cultures differs notably from that of tissue-embedded cells. Furthermore, in cases where the substrate surface properties (*e.g.*, its chemistry, texture) do not meet the cells' most basic anchoring requirements, the cells tend to aggregate or die. Apart from keeping a cell in place, the interaction with extracellular matrix (ECM) components serves a multitude of other vital purposes (*e.g.*, gene expression, migration, proliferation, differentiation) (Frantz *et al.*, 2010; Mecham, 2012; Mouw *et al.*, 2014). Besides the ECM's chemical composition and biochemistry, its physical (*e.g.*, stiffness) and spatial (*e.g.*, surface topography) properties are considered potent modulators of cell fate (Akhmanova *et al.*, 2015). Therefore, any aggregation phenomenon or cell detachment can be considered a direct consequence of the cells' struggle for survival and functional identity.

Recently, three-dimensional culture models are on the rise, particularly in the context of tissue engineering and controlled-release drug delivery (Breslin and O'Driscoll, 2013; Comley, 2010; Haycock, 2010; Huh *et al.*, 2011; Liechty *et al.*, 2010). A collection of 3D cell culture information sources can be found at www.3dcellculture.com. 3D models are based on the idea of mimicking the ECM, thereby gaining better control over tuning intercellular adhesion, cell fate and culture architecture. In the context of microelectrode array (MEA) electrophysiology (Kim *et al.*, 2014), a 3D matrix would not only allow neurons to interconnect in a more natural way, but attenuate sudden changes in the microenvironment and increase the number of neighbors, computational units and thus functional network complexity.

Some popular strategies for establishing a more organotypic-like 3D cell culture are the use of rigid scaffolds (Carletti *et al.*, 2011) (*e.g.*, microbeads (Frega *et al.*, 2014) or protein-binding polymer scaffolds (Greiner *et al.*, 2012)) coated with ECM-like adhesion and signaling factors, the direct embedding of cells into detergent-extracted ECM scaffolds (Ott *et al.*, 2008) or functionalized hydrogels. Hydrogels are network-like polymers with high water content (Buwalda *et al.*, 2014). Due to their softness and 3D meshwork, cells can engage in a more tissue-mimetic cell-matrix interaction. Apart from their biomedical use (*e.g.*, contact lenses, wound dressings, drug delivery devices (Caló and Khutoryanskiy, 2015)), hydrogels have found their way into cell culture labs (Altmann *et al.*, 2009; Andersen *et al.*, 2015; Tibbitt and Anseth, 2009) and tissue engineering (Baroli, 2007;

Kim *et al.*, 2011; Leal-Egaña *et al.*, 2013; Hunt *et al.*, 2014). In the latter context, they serve as circuit reconstruction scaffolds for the timed orchestration of events in (neuro)development, as drug delivery devices or as cell encapsulation constituents for implantation (Aurand *et al.*, 2012a, 2012b; Carballo-Molina and Velasco, 2015; McMurtrey, 2015). There are several categories of gelling agents to choose from. Among those are purified peptides or (glyco)proteins of animal origin (*e.g.*, egg white (Kaipparettu *et al.*, 2008), proteoglycans, fibronectin, laminins, collagens or a mix of basal lamina proteins (Yurchenco, 2011)), artificial protein mixes (Zhao and Zhang, 2006), microbial- (*e.g.*, gellan gum, xanthan gum), algae- (*e.g.*, carrageenans, alginates, agarose) or plant-derived polymers (*e.g.*, guar gum, locust bean gum, tragacanth) or polymers of completely synthetic origin (Kopecek, 2002; Lei and Schaffer, 2013). Although synthetic gels are usually expensive, they can be produced in a defined stoichiometry without impurities and their physico-chemical properties be tailored to the cells' needs, thereby giving more reproducible results. In contrast, natural food-grade gelling agents are relatively inexpensive and readily available, but can vary in composition and carry production-related residues. These may need to be removed beforehand (*e.g.*, by simple filtering or a solid phase extraction (SPE) process). Depending on their chemical and mechanical properties (*e.g.*, wettability, presence of biofunctional anchors, rigidity, micro- and nano-topography, porosity) as well as on their net charge at physiological pH, most gels require the addition of cell-specific anchoring and signaling factors (*e.g.*, laminins, fibronectin) to mask unfavorable properties and to support cellular attachment and differentiation.

Apart from its physicochemical properties and biochemistry, the decision on whether a gelling agent may be suitable for cell embedment depends on several other, more practical factors. Its gelling propensity should be predictable and not be affected by the ingredients of a cell culture medium. Similarly, if the gelling mechanism is ion-dependent, the medium composition should not be unfavorably altered through the gelling process. It should gel at or below physiological temperatures to not cause the denaturing of the proteins in the medium. If the gelling process can be controlled, *e.g.*, through light (*e.g.*, by photocrosslinking), pH (Dou *et al.*, 2012), electric fields or charges, redox agents, mechanical manipulation (Pek *et al.*, 2008), particular cross-linking agents (*e.g.*, enzyme-initiated) or temperature, the mechanism and reaction by-products should not affect its cytocompatibility. Equally, a gel should not be metabolized by the cells or be degraded by excreted metabolites over time. In addition, a gelling agent should be sterilizable without altering its gelling properties.

This study aimed at the testing and comparison of affordable gelling agents of non-animal origin as extracellular matrix substitutes both for establishing 3D-like neural networks

on microelectrode arrays (MEAs) and for stabilizing the local microenvironment against physicochemical fluctuations (*e.g.*, handling artifacts such as vibration, mechanical impact, mixing, convection, rapid change of diffusion gradients). Besides temperature, common critical variables in cell culture are osmolality and pH, which can quickly change in small medium volumes (Heo *et al.*, 2006). Osmotic and pH drift are not only due to evaporation, but also to metabolic exchange, thereby altering the local medium and ECM composition quickly (Yarmush and King, 2009). In this context, a gel is expected to act as a sponge-like buffer against rapid changes in environmental parameters.

2 Materials

2.1 Preparation and plating of rat cortical cell suspensions

All experiments involving animals were carried out in accordance with the guidelines established by the European Communities Council (Directive of November 24th, 1986) and approved by the National Council on Animal Care of the Italian Ministry of Health. Pregnant Sprague Dawley rats (CD IGS, Charles River) were anesthetized and sacrificed by cervical dislocation 18 days after conception. Following standard tissue dissociation protocols (Banker and Goslin, 1998), embryos (E17/E18) were harvested and put on ice in Hank's balanced salt solution (HBSS, ThermoFisher) and decapitated. After removing the meninges, the cortices were extracted, minced and transferred to fresh HBSS and dissociated into single cells using 0.25% (w/v) trypsin in HBSS buffer. After incubation for 10 min at 37 °C, the trypsin was deactivated by 0.25 mg/ml soybean trypsin inhibitor along with 0.01% (w/v) DNase (Sigma DN25). Cell suspensions were prepared by sequential trituration (15–20 times) using three fire-polished Pasteur pipettes with decreasing diameters. Cells were then centrifuged at 200 g for 5 min and the pellets were resuspended in Neurobasal medium (NBM) containing 2% B-27 serum-free supplement, 1 mM penicillin/streptomycin and 2 mM Glutamax (all ThermoFisher). MEAs (30/500iR, Multi Channel Systems) carrying an OD 24 mm glass ring as a culture medium container were autoclaved and subsequently hydrophilized beforehand by a short O_2 plasma treatment (0.3 mbar, 1 min, 60 W, 2.45 GHz, Diener plasma GmbH) and thereafter were coated with a 10 µl drop of a poly-D-lysine (PDL) (0.1 mg/ml, Sigma P6407) and laminin (5 µg/ml, Sigma L2020) mix in ultrapure sterile water. Drops were allowed to dry in the vacuum of the plasma chamber. Soluble coating components were thoroughly rinsed with ultrapure sterile water. The MEAs were dried again in the vacuum of the plasma chamber before plating the cells or depositing the (cell-laden) gels. Protected against evaporation by PDMS caps without perfusion functionality (Blau *et al.*, 2009), cells were allowed to settle for less than 10 min in a humidified (92–95% RH) incubator at 37 °C in a 5% CO_2 in air atmosphere before adding pre-warmed cell culture medium.

2.2 Culture and perfusion medium

Cultures were plated and grown in above-mentioned NBM. For gel benchtop experiments and control cultures, the medium contained a suitable pH buffer. The pH of the buffered media had been adjusted to 7.4 at room temperature without preconditioning it to ambient CO_2 levels (0.038%). The buffers (Bufferall, Sigma B8405; L-histidine, Fluka 53370; HEPES, Sigma H0887) were mixed with the NBM to give a final concentration of 2–20 mM. These buffers were found to stabilize pH equally well at ambient CO_2 levels as well as in control cultures that were kept in a humidified 5% CO_2 incubator.

2.3 Gelled medium

Where necessary, powders were sterilized either by the UV light of a cell culture workbench, dry autoclavation for 120 min at 160 °C or by their dispersion in 70% ethanol and subsequent drying at 120 °C for 60 minutes. Food-grade gelling agents (ι-carrageenan, Fluka 22045; κ-carrageenan, Fluka 22048; gellan gum, Sigma G1910; guar gum, Sigma G4129; locust bean gum, Sigma G0753; sodium alginate (medium viscosity), Sigma, A2033; tragacanth, Sigma, G1128; xanthan gum, Fluka 95465) were added to separate NBM batches at 1–4% (w/v) with or without laminin (5 µg/ml, Sigma L2020). Gels were ultrasonicated in closed 15 ml Falcon tubes at room temperature for less than one minute. A 6 nm pore solid phase extractor (Empore C18-SD cartridge) was used to remove opaqueness from turbid guar gum and locust bean gum batches. Where necessary, gels of higher viscosities were handled by a more powerful Combitip Multipette®. For direct cell embedment into gels, 50–100 µl of the neural cell suspension were mixed into a 1.5 ml gel aliquot by careful trituration with a 1 ml pipette to give a final cell density of about 150 000 cells per aliquot. 200 µl aliquots were transferred onto the PDL/laminin pre-coated cell culture substrates (24-well plates). In the other two cases (protective gel top-layer or cells on top of a gel), cells were plated at a density of about 60 000 cells per culture container. Culture containers were kept in a humidified 5% CO_2 incubator. Well plates were protected against evaporation by Parafilm, control MEAs by a PDMS cap without perfusion functionality (Blau *et al.*, 2009). For the long-term perfusion study, the gels had been pre-deposited onto the PDL/laminin-coated MEAs. 50 µl of a cortical cell suspension were plated on top of a guar gel (1% w/v) containing a higher concentration of laminin (15 µg/ml) to result in a final cell density of 365 000 cells per culture. Cells were allowed to migrate into the gel and to settle on the MEA substrate surface while being stored in the incubator. MEA cultures were protected against evaporation by above mentioned PDMS caps. At 24 DIV, caps were exchanged with perfusion caps (Saalfrank *et al.*, 2015) before the MEAs were transferred to the perfusion setup on the lab bench for long-term electrophysiology and imaging.

2.4 Culture maintenance

All cultures were kept in a humidified (92–95% RH) incubator at 37 °C in a 5% CO_2 in air atmosphere. Cultures in 24-well plates and on MEAs contained 200 µl gel with a 500 µl supernatant medium layer. Depending on the color of the phenol red pH indicator, up to half of the medium (250 µl) was exchanged once a week. One of the MEA guar gum gel cultures was inserted into the perfusion platform at 24 DIV. Before its transfer, the supernatant was replaced by chemically buffered NBM.

2.5 Perfusion parameters

The perfusion culture was kept at 35.5–36.5 °C with an un-controlled but constant vertical T-gradient through the culture dish. It was continuously perfused. Buffered NBM was stored at room temperature in a 100 ml glass bottle with a PDMS membrane (∅ 30 mm, 3 mm thick) in its cap. A 5 mm thick silicone oil (Aldrich 317667) layer floating on the medium attenuated evaporation into the head space of the bottle. A custom-made stepper motor-driven (Blau and Ziegler, 2001) syringe pump had been connected to the chamber outlet tube to control the perfusion volume. Medium from the medium supply bottle flowed gravity-driven into the chamber, thus maintaining a slight overpressure. Its magnitude was dictated by the relative height of the supply medium level with respect to the cell culture (~300 mm). Perfusion rates were adjusted to ⩽250 µl/day.

2.6 Multichannel MEA electrophysiology and spike train analysis

Extracellular signals were recorded and processed by a commercial 60-channel, 1 Hz–3 kHz bandpass filter-amplifier data acquisition system (25 kHz sampling rate per channel) (Multi Channel Systems, MEA60-Up). The MEA socket in its base plate featured a resistive heating element and a Pt-100 temperature sensor. An external T-control unit (Multi Channel Systems, HC-1) kept the temperature of the socket surface at ⩽ 36.5 °C. The amplifier was mounted onto a fixed, custom-made stage of an inverted microscope (Zeiss Axiovert 200). A grounded metal cap with a central hole for illumination was placed onto the amplifier as a Faraday shield. Additionally, two grounded microclips (Conrad 102407) were connected to both metal syringe needles at the inlet and outlet septa, respectively. A grounded aluminum foil wrapped around the tubing reduced noise picked up by the fluid lines. Further methodological details on the overall setup can be found in a recent report (Saalfrank *et al.*, 2015).

To reduce data file size, only upward (positive) and downward (negative) spike cut-outs from each of the 54 recording electrodes were stored in one or five minute packets. They consisted of 5 ms pre-spike and 5 ms post-spike fragments after the first threshold crossing at ±5.5 StDev from peak-to-peak noise. Only downward threshold-crossings were analyzed. Spike trains were transformed into time stamps using NeuroExplorer (Nex Technologies). After automatically identifying and removing simultaneous timestamps from all channels (NotSync function in NeuroExplorer) that occurred on at least four reference channels within ±10 ms due to electrical or handling artefacts (*e.g.*, the temporary removal of the Faraday shield), resultant datasets were sequentially merged to give 12-h timestamp packets for further analysis. Cumulative activity on all available channels was calculated by counting the number of timestamps within subsequent one-minute bins. Most data processing steps were automated through scripts. Numbers were transferred to Microsoft Excel for plotting.

2.7 Imaging

Still images were collected with an inverted Leica DMILED microscope equipped with a Leica DFC420 C digital camera. Time-lapse pictures were taken by a remote-controlled (PSRemote, Breeze Systems) Canon G2 digital camera attached to the camera port of the Zeiss Axiovert 200 microscope. To reduce light-induced degradation of the chemical buffer (Lepezuniga *et al.*, 1987), a high-intensity LED light (IKEA Jansjö) was switched on by a programmable relay (Conrad Electronics C-Control) for 30 s within a time-lapse interval of three minutes. During this period, a picture was taken. Regions of interest (ROIs) were cropped by using the XnView software.
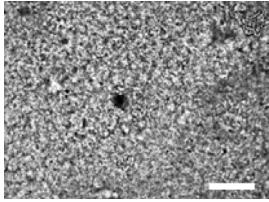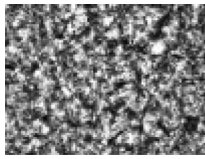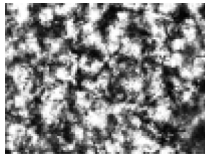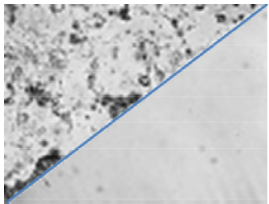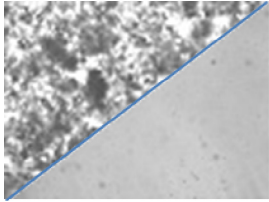
3 Results and discussion

To provide a cost-efficient three-dimensional ECM-like scaffold that attenuates diffusion, thereby stabilizing the chemical microenvironment, eight different microbial-, plant- or algae-derived gelling agents were selected and tested for their gelling properties, their transparency and cytocompatibility in serum-free, but supplemented (B27, pen/strep, Glutamax) Neurobasal medium with or without laminin at physiological pH (~7.4) within a temperature range of 25 °C to 37 °C, namely ι- and κ-carrageenan, gellan gum, guar gum, locust bean gum, sodium alginate, tragacanth and xanthan gum. Gelling agents that required gelling temperatures above 37 °C (*e.g.*, agarose, food-grade gelatin, amylopectin) or that altered the pH of the cell culture medium (*e.g.*, karaya gum) were not further considered.

Powder sterilization by UV irradiation was unreliable due to the limited penetration depth of the radiation and shadow effects. In contrast, both dry sterilization at 160 °C and powder dispersion in 70% ethanol and subsequent drying were effective. In a pre-screening step, viscosities for a given weight-per-volume percentage were found to vary with the type and composition of the cell culture medium (*e.g.*, minimum essential medium (MEM), Dulbecco's modified Eagle medium (DMEM); data are not shown).

For the selected gels, effective gelling percentages in Neurobasal medium without any additives were found to stay within a range of 1% to 4%. A viscosity was considered suitable for cell embedment if cells could be dispersed into the gel and stay buoyant instead of settling on the bottom of the cell culture container. Usually, this was the concentration when a gel started to lose it fluidity. Cells could be dispersed easily in low-viscosity gels, but tended to precipitate on the culture substrate to result in quasi-2D cultures. In contrast, high-viscosity gels did not allow for homogeneous cell dispersal anymore. Cells plated directly onto the surface of high-viscosity gels rarely spread into the gel. Therefore, the best strategy to distribute cells homogeneously within a gel was to mix them with the gelling agent during the gelling process or plate them onto a medium-viscosity gel and allow for their gravity-assisted migration into the gel.

Relevant properties and effective gelling concentrations of the investigated gels are listed in Table 1. With the exception of ι-carrageenan, all gels where 'self-healing' when mechanically perturbed; gels would fuse at any created gaps without leaving a border that would show as a change in the refractive index under the microscope. As the phase contrast images show, each gel – with the exception of filtered guar gum and locust bean

Table 1. Properties and textures of the investigated gels. The 200 μm scale bar (see *ι*-carrageenan) applies to all images. Note: some dots and diagonal stripes common in all images (notable for guar and locust bean gum) are artefacts (due to dirt in the optical path of the microscope).

Gelling agent	Viscosity change with temperature from 25 °C to 37 °C	Transparency	Effective concentration [%] (w/v)	Properties	Appearance
ι-carrageenan from red algae (Fluka/Sigma, C1138)	highly positive within a few minutes	clear, slightly textured	2	Anionic linear sulfated polysaccharide forms soft gels in the presence of calcium ions; solid, no fluidity, no self-repair (leaves interface gaps when broken apart)	
κ-carrageenan from red algae (Fluka/Sigma, 22048)	positive within a few hours	milky and textured	2–4	Sulfated polysaccharide; forms rather solid gels in the presence of potassium ions with very low fluidity	
Gellan gum from *Sphingomonas eldea* (Sigma, G1910)	positive within a few minutes	slightly opaque, but strongly textured	3	Anionic polysaccharide, a divalent cation-dependent hydrocolloid (dispersion of aggregated gel clusters)	
Guar gum from guar beans (Sigma, G4129)	highly positive within a few minutes	unfiltered: slightly opaque with turbid irregular inclusions; almost clear after filtering	1–3	Polysaccharide, that forms a rather solid, self-repairing gel in the presence of Ca^{2+} (or borax); contains plant residues, which can be filtered by SPE with some decrease in its viscosity	
Locust bean gum from *Ceratonia siliqua* seeds (Sigma, G0753)	highly positive within a few minutes	unfiltered: slightly opaque with turbid irregular inclusions; rather clear after filtering	1–3	Galactomannan hydrocolloidal polysaccharide forms medium viscous, slightly fluid, self-repairing gels; contains plant residues, can be filtered by SPE	
Sodium alginate from brown algae (medium viscosity) (Sigma, A2033)	positive within several hours	almost clear with characteristic texture	4	A straight-chain, hydrophilic, colloidal, polyuronic acid, divalent cation (Ca^{2+})-dependent, medium viscous, slightly fluid	
Tragacanth (Sigma, G1128)	highly positive within a few seconds	slightly opaque, strongly textured	4	Complex mixture of polysaccharides, which forms a colloidal hydrosol	
Xanthan gum from *Xanthomonas campestris* (Sigma, G1253)	highly positive within a few minutes	opaque, slightly textured	1	Anionic polysaccharide, which forms a hydrophilic colloid	

DOSSIER

gum – had a typical morphology on a similar length scale of cells. Apart from insufficient homogenization, these textures may be attributed to their different tertiary polymer structures and the resulting aggregation tendencies. Locust bean gum and guar gum furthermore contained production-related plant residues. Because their size was similar to that of cells, it was difficult to identify the details of a gel-embedded neural network. Residues could be removed by passing the gel through a solid-phase extraction (SPE) cartouche to yield largely transparent, homogeneous and sterile gels at the cost of reducing their viscosity. This was due to the chosen pore size of 6 nm, which was too small to let the highly crosslinked portions pass through. The same clearing process could not be applied to the other gels. Either just the medium or the entire gel would pass unchanged the strainer.

For 1% (w/v) mixtures in Neurobasal medium without laminin, viscosities were found to increase in the following order: gellan gum ≈ κ-carrageenan ≈ tragacanth ≈ sodium alginate (partially gelled) < locust bean gum < guar gum < ι-carrageenan < xanthan gum. Transparency decreased in the following order: ι-carrageenan (clear) > sodium alginate (almost clear) ≈ guar gum (filtered: translucent) ≈ locust bean gum (filtered: translucent) > tragacanth (translucent) > gellan gum (cloudy) ≈ locust bean gum (unfiltered: milky) ≈ guar gum (unfiltered: milky) > κ-carrageenan (milky) > xanthan gum (milky). In a 24-well plate pre-screening study, different cell plating strategies were compared: (1) mixing the cells directly into the gel during the gelation process, (2) pre-deposition of a gel onto the cell culture substrate and plating of neurons on top of it or (3) plating of cells on the substrate surface followed by their protective coating with a gel against flow-induced fluctuations in their microenvironment. In all cases, a 500 µl medium overlay was added. Embedded neurons survived and differentiated only in laminin-supplemented guar gum (Fig. 1a), locust bean gum (Fig. 1b) and xanthan gum. Neurons plated on top of a 200 µm gellan gum layer without laminin partially migrated into the gel and differentiated as well (Fig. 1c). Gellan gum apparently provides some of the required ligands to support cell survival and differentiation without the need for supplemented cell adhesion and differentiation factors. Pre-plated neurons covered by sodium alginate right after plating survived and differentiated as well (Fig. 1D).

However, neurons directly embedded into laminin-supplemented sodium alginate did not differentiate. Although ι-carrageenan featured very high transparency and, like κ-carrageenan, high viscosity, cells did not differentiate under the chosen experimental conditions. Both gels were therefore not further considered as 3D culture matrices. Equally, tragacanth and xanthan gum, despite their potential of hosting cells, were not further investigated due to their higher opaqueness, which limited their usefulness in network imaging studies. In all other plating scenarios, no cell differentiation could be observed. This may be due to the chosen laminin concentration of 5 µg/ml. While this concentration is effective in supporting cell anchoring and differentiation on 2D substrates, it apparently was not sufficient for a 3D environment as the predominant clustering of cells within a gel suggested. As a result, costs for establishing 3D cultures based on the tested microbial-, algae- or plant-derived gelling agents increase notably if laminin
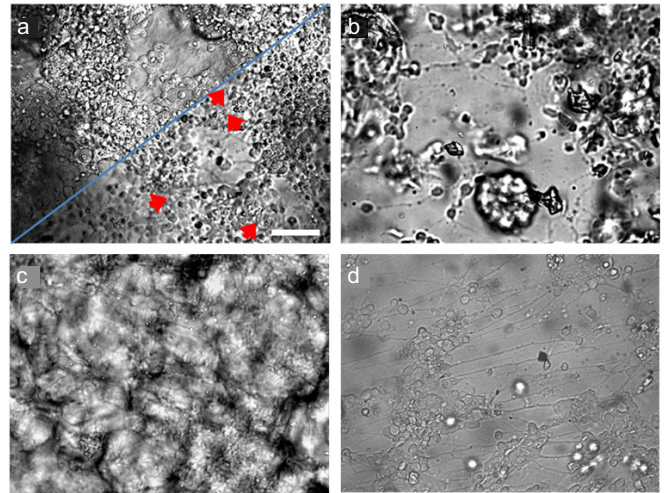

Fig. 1. Gel-embedded, gel-invading and gel-covered cortical neurons at 4 days *in vitro* (DIV). (a) Filtered guar gum gel (< 3%) containing laminin with well differentiated 2D cell carpet at the bottom of the culture well (top left) and embedded neural clusters with a few clearly visible axonal connections in between (red arrows) about 100 µm above the bottom (bottom right). (b) Unfiltered locust bean gum gel (3%) containing laminin with low density network of differentiated neurons at the bottom and cell clusters as well as plant fragments in focus. (c) Center of a cloudily structured gellan gum gel (3%) layer without any added adhesion factors shows less densely, but clearly differentiated neurons interconnecting with less differentiated clusters. Neurons, originally seeded on top of the gel, had sunk or migrated into and homogeneously distributed within the gel. (d) Neurons covered directly after seeding by a sodium alginate gel (4%) with intercalated laminin have differentiated comparable to control cultures (not shown). In all images, undifferentiated cells appear as bright round spheres. Scale bar: 50 µm (a, b, d) and 100 µm (c).

cannot be substituted for alternative, less expensive cell adhesion and differentiation factors.

In a follow-up experiment, a 1% guar gum gel with a three-time higher laminin concentration was chosen to test the long-term cell viability and electrophysiology of gel-embedded cortical neurons. The culture was kept in an incubator before being mounted in a 60-channel amplifier at 24 days *in vitro* (DIV). Its activity was recorded from 24 DIV to 79 DIV from an average of 36 channels out of 54 active channels (Fig. 2). The culture was imaged at constant illumination over the same period. Over time, the culture had been exposed to three different chemical buffer systems (Bufferall, HEPES and L-histidine; all at 10 mM). Details on the experimental setup are given in a recent report (Saalfrank *et al.*, 2015). Details of the cortical network morphology are hardly discernible due to the non-soluble residues in the unfiltered gel (Fig. 3).

The challenges and benefits of culturing cells in gels, particularly in microfluidics, have been discussed by other research groups before (Dhaliwal, 2012; Geckil *et al.*, 2010; Thiele *et al.*, 2014; Tibbitt and Anseth, 2009). Unfortunately, few of the suitable gels are sufficiently clear and homogeneous and thus tend to obscure optical access to the cells. Also in our case, the unfiltered guar gum was not clear, but translucent and contained cell-sized residues making it difficult to discern cell culture morphology. In adjunct experiments, we observed
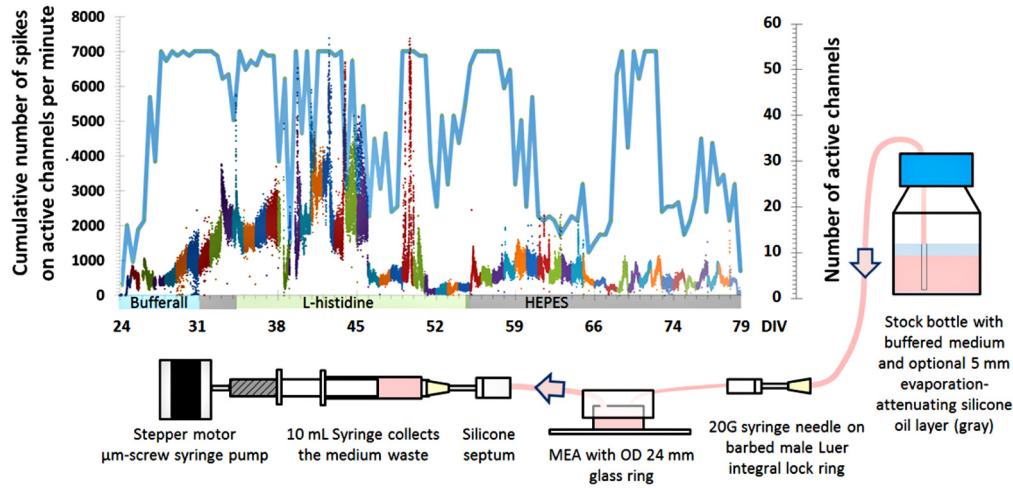
Fig. 2. Activity evolution and number of active recording channels for a cortical culture in guar gum in the perfusion system at ambient air over a period of 55 DIVs. Each dot represents the cumulative activity (sum of recorded action potentials) during one minute time bins on all active channels (blue trace). Each day is depicted with a different dot color. Buffer types are color-coded along the *x*-axis. The perfusion configuration is sketched below the graph.
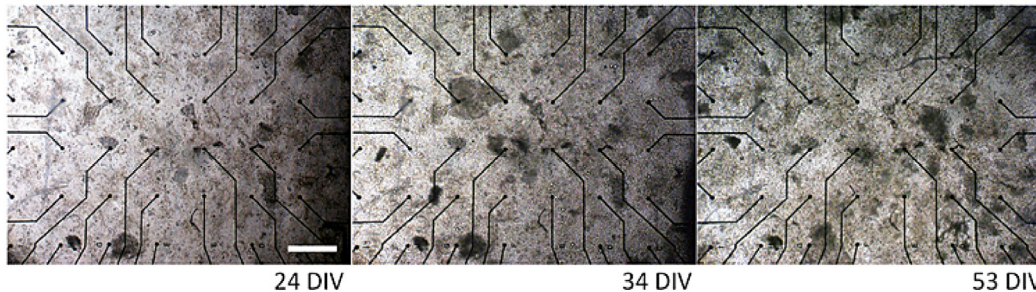

Fig. 3. Comparative image collage of macroscopic gel- and network-morphology in the cortical gel culture at different DIVs in the perfusion setup. Due to the non-soluble/non-gelling residues (gray islands), network morphology at 24, 34 and 53 DIV is not easily discernible. Electrode spacing and scale bar: 500 μm.

that 2D cultures suffered irreversibly if daily perfusion rates repetitively exceeded the overall cell culture volume (data not shown). While perfusion throughput reached these volumes in the cortical 3D gel culture at least once, the gel seems to have attenuated its detrimental effect as the recorded activity elucidates. It supported the stabilization of a local microenvironment and protected the culture from drying out despite occasional flush perfusion due to unexpected leakage through the perfusion cap and subsequent emptying of the medium supply followed by an accumulation of air in the cap thereafter.

This screening study on a selection of readily available gelling agents for the creation of cell culture scaffolds stated some of the necessary requirements for and desirable features of such matrices. Combining 3D culture techniques with other experimental paradigms such as microelectrode array electrophysiology and time-lapse imaging promises to not only enhance culture survival at ambient conditions, but to extend the range of experimental possibilities for *in vitro* studies in general.

References

Akhmanova M, Osidak E, Domogatsky S, Rodin S, Domogatskaya A. 2015. Physical, Spatial, and Molecular Aspects of Extracellular Matrix of In Vivo Niches and Artificial Scaffolds Relevant to Stem Cells Research. *Stem Cells Int.* Article ID 167025.

Altmann B, Welle A, Giselbrecht S, Truckenmuller R, Gottwald E. 2009. The famous versus the inconvenient – or the dawn and the rise of 3D-culture systems. *World J. Stem cells* 1: 43–48.

Andersen T, Auk-Emblem P, Dornish M. 2015. 3D Cell Culture in Alginate Hydrogels. *Microarrays.* 2: 133–161.

Aurand ER, Lampe KJ, Bjugstad KB. 2012a. Defining and Designing Polymers and Hydrogels for Neural Tissue Engineering. *Neurosci. Res.* 3: 199–213.

Aurand ER, Wagner J, Lanning C, Bjugstad KB. 2012b. Building Biocompatible Hydrogels for Tissue Engineering of the Brain and Spinal Cord. *J. Funct. Biomat.* 4: 839–863.

Banker G, Goslin K 1998, Culturing nerve cells, 2 ed. Cambridge: The MIT Press.

Baroli B. 2007. Hydrogels for tissue engineering and delivery of tissue-inducing substances. *J. Pharm. Sci.* 9: 2197–2223.

Blau AW, Ziegler CM. 2001. Prototype of a novel autonomous perfusion chamber for long-term culturing and in situ investigation of various cell types. *J. Biochem. Biophys. Methods* 1: 15–27.

Blau A, Neumann T, Ziegler C, Benfenati F. 2009. Replica-molded poly(dimethylsiloxane) culture vessel lids attenuate osmotic drift in long-term cell culturing. *J. Biosci.* 1: 59–69.

Breslin S, O'Driscoll L. 2013. Three-dimensional cell culture: the missing link in drug discovery. *Drug Discov. Today* 5–6: 240–249.

Buwalda SJ, Boere KWM, Dijkstra PJ, Feijen J, Vermonden T, Hennink WE. 2014. Hydrogels in a historical perspective: From simple networks to smart materials. *J. Control Release* 190: 254–273.

Caló E, Khutoryanskiy VV. 2015. Biomedical applications of hydrogels: A review of patents and commercial products. *Eur. Polym. J.* 65: 252–267.

Carballo-Molina OA, Velasco I. 2015. Hydrogels as scaffolds and delivery systems to enhance axonal regeneration after injuries. *Front. Cell. Neurosci.*: 13.

Carletti E, Motta A, Migliaresi C. Scaffolds for tissue engineering and 3D cell culture. In: Haycock JW, ed. 3D Cell Culture Humana Press, 2011.

Comley J. 2010. 2D Cell Culture: easier said than done! Summer 10. Drug Discovery World Summer 2010 (ddw-online.com) pp. 24–41.

Dhaliwal A. 2012. Three dimensional cell culture: A review. *Materials and Methods* 2: 162.

Dou X-Q, Yang X-M, Li P, Zhang Z-G, Schonherr H, Zhang D, Feng C-L. 2012. Novel pH responsive hydrogels for controlled cell adhesion and triggered surface detachment. *Soft Matter* 37: 9539–9544.

Frantz C, Stewart KM, Weaver VM. 2010. The extracellular matrix at a glance. *J. Cell Sci.* 24: 4195–4200.

Frega M, Tedesco M, Massobrio P, Pesce M, Martinoia S. 2014. Network dynamics of 3D engineered neuronal cultures: a new experimental model for *in vitro* electrophysiology. *Sci. Rep.* 5489.

Geckil H, Xu F, Zhang X, Moon S, Demirci U. 2010. Engineering hydrogels as extracellular matrix mimics. *Nanomedicine* 3: 469–484.

Greiner AM, Richter B, Bastmeyer M. 2012. Micro-Engineered 3D Scaffolds for Cell Culture Studies. *Macromol. Biosci.* 10: 1301–1314.

Haycock JW. 3D cell culture: A review of current approaches and techniques. T 3D Cell Culture, 2010.

Heo YS, Cabrera LM, Song JW, Futai N, Tung YC, Smith GD, Takayama S. 2007. Characterization and resolution of evaporation-mediated osmolality shifts that constrain microfluidic cell culture in poly(dimethylsiloxane) devices. *Anal. Chem.* 3: 1126–1134.

Huh D, Hamilton GA, Ingber DE. 2011. From 3D cell culture to organs-on-chips. *Trends Cell Biol.* 12: 745–754.

Hunt JA, Chen R, van Veen T, Bryan N. 2014. Hydrogels for tissue engineering and regenerative medicine. *J. Mater. Chem. B* 33: 5319–5338.

Kaipparettu BA, Kuiatse I, Chan BT-Y, Kaipparettu MB, Lee AV, Oesterreich S. 2008. Novel egg white-based 3-D cell culture system. *BioTechniques* 2: 165–168.

Kim B-S, Park I-K, Hoshiba T, Jiang H-L, Choi Y-J, Akaike T, Cho C-S. 2011. Design of artificial extracellular matrices for tissue engineering. *Prog. Polym. Sci.* 36: 238–268.

Kim R, Joo S, Jung H, Hong N, Nam Y. 2014. Recent trends in microelectrode array technology for in vitro neural interface platform. *Biomed. Eng. Lett.* 2: 129–141.

Kopecek J. 2002. Polymer chemistry: swell gels. *Nature* 6887: 388–389, 391.

Leal-Egaña A, Díaz-Cuenca A, Boccaccini AR. 2013. Tuning of Cell–Biomaterial Anchorage for Tissue Regeneration. *Adv. Mater.* 29: 4049–4057.

Lei Y, Schaffer DV. 2013. A fully defined and scalable 3D culture system for human pluripotent stem cell expansion and differentiation. *Proc. Natl. Acad. Sci. USA* 52: E5039–E5048.

Lepezuniga JL, Zigler JS, Gery I. 1987. Toxicity of Light-Exposed HEPES Media. *J. Immunol. Methods* 1: 145–145.

Liechty WB, Kryscio DR, Slaughter BV, Peppas NA. 2010. Polymers for drug delivery systems. *Ann. Rev. Chem. Biomol. Eng.* 149–173.

McMurtrey RJ. 2015. Novel advancements in three-dimensional neural tissue engineering and regenerative medicine. *Neural Regener. Res.* 3: 352–354.

Mecham RP. 2012. Overview of extracellular matrix. Curr. Protoc. Cell Biol. John Wiley & Sons, Inc..

Mouw JK, Ou G, Weaver VM. 2014. Extracellular matrix assembly: a multiscale deconstruction. *Nat. Rev. Mol. Cell Biol.* 12: 771–785.

Ott HC, Matthiesen TS, Goh S-K, Black LD, Kren SM, Netoff TI, Taylor DA. 2008. Perfusion-decellularized matrix: using nature's platform to engineer a bioartificial heart. *Nat. Med.* 14: 213–221.

Pek YS, WanAndrew CA, Shekaran A, Zhuo L, Ying JY. 2008. A thixotropic nanocomposite gel for three-dimensional cell culture. *Nat. Nanotechnol.* 11: 671–675.

Saalfrank D, Konduri AK, Latifi S, Habibey R, Golabchi A, Martiniuc AV, Knoll A, Ingebrandt S, Blau A. 2015. Incubator-independent cell-culture perfusion platform for continuous long-term microelectrode array electrophysiology and time-lapse imaging. *R. Soc. Open Sci.* 2: 150031.

Thiele J, Ma Y, Bruekers SMC, Ma S, Huck WTS. 2014. 25th anniversary article: designer hydrogels for cell cultures: A materials selection guide. *Adv. Mater.* 1: 125–148.

Tibbitt MW, Anseth KS. 2009. Hydrogels as extracellular matrix mimics for 3D cell culture. *Biotechnol. Bioeng.* 4: 655–663.

Yarmush ML, King KR. 2009. Living-cell microarrays. *Ann. Rev. Biomed. Eng.*: 235–257.

Yurchenco PD. 2011. Basement membranes: Cell scaffoldings and signaling platforms. *Cold Spring Harb. Perspect. Biol.* 2.

Zhao X, Zhang S. 2006. Molecular designer self-assembling peptides. *Chem. Soc. Rev.* 11: 1105–1110.